

SciEn Conference Series: Engineering Vol. 3, 2025, pp 399-404

https://doi.org/10.38032/scse.2025.3.109

Micromechanical FE Analysis of Unidirectional E-Glass Fiber Reinforced Epoxy Composite

A. B. M. Tareq Rahman Sakib, Md. Shahidul Islam*, Md. Jamiun Noor Shadman

Department of Mechanical Engineering, Khulna University of Engineering & Technology, Khulna-9203, Bangladesh

ABSTRACT

Composite materials, formed by consolidating two or more materials with distinct physical and chemical characteristics, exhibit unique properties which is not found in their individual components. Extensive research has been conducted using micromechanical approaches to analyze unidirectional (UD) composites, demonstrating their efficacy in addressing composite material-related challenges. This study employed micromechanical finite element analysis (FEA) to estimate the effective properties of UD E-glass fiber reinforced composites. The analysis started with a random distribution of fibers within the representative volume element (RVE), followed by two regular distributions: hexagonally packed and square packed. An algorithm using Python generated the random fiber distribution within RVE, considering the fibers have perfectly circular cross-sections. The fiber volume fraction within the RVE was varied from 0.1 to 0.5, and the effects on the properties of the composite were evaluated. Rule of Mixtures (ROM) was employed to determine the longitudinal modulus and Poisson's ratio, while Halpin-Tsai equation was applied for the transverse modulus and shear modulus. These analytical solutions were then compared with FEA results. It is observed from the present analysis that with fiber volume fraction increased from 10% to 50% the effective properties also increased, for instance E₁₁ for random distribution increased from 11.76 GPa to 39.5 GPa, except the Poisson's ratio, which decreased to 0.25 from 0.32. Comparing with the other distribution, Random distribution exhibited superior load carrying capacity.

Keywords: FEA, Composite, E-Glass, ABAQUS, Micromechanical



Copyright @ All authors

This work is licensed under a <u>Creative Commons Attribution 4.0 International License</u>.

1. Introduction

Composite materials, essential in engineering for their superior performance, are widely used in automobiles, spacecraft, and sports equipment. Unidirectional composites are specifically valued and considered transversely isotropic homogeneous materials in many applications [1]. These composites possess distinctive characteristics, meeting high demand more efficiently and profitably than regular materials. Advantages include stable homogeneous properties, reduced production costs, decreased weight, and improved impact and fatigue resistance [2]. Traditional materials often require extra strength in non-load-bearing directions, adding unnecessary cost and weight to structures [3]. Homogenization of elastic properties for composites is a very important phase of the process of any composite material structure. For instance, micromechanical model equations are proposed by Chamis [4], and the asymptotic mean-field homogenization are proposed by Mori-Tanaka [5]. FEA techniques including the RVE homogenization method are more precise, extensively used to forecast the effective elastic property of composites, and have emerged as the standard procedure for dealing with composite materials [6, 7]. Utilizing micromechanics, Bednarcyk, B.A. and Arnold forecasted deformation and failure for titanium composites with longitudinal reinforcement [1]. Kok, de J.M.M. and Meijer, H.E.H studied the effect of fiber volume fraction and test temperature for the effective transverse mechanical properties for epoxy matrix embedded with glass fiber by both experimental and numerical methods [8]. Christoph Unterweger, Oliver Brüggemann, and Christian Fuerst studied the influence of many kinds of fibers and their

volume fractions for the short fiber-reinforced polypropylene composites [9]. Sonparote PW and Lakkad SC investigated the various mechanical properties (tensile, compressive, flexural etc.) of a hybrid composite [10]. Lamon, J, determined the mechanical behavior of brittle- matrix composites on the basis of micro mechanics approaches [11]. Sun, H., Di, S., Zhang, N. and Wu, C. proposed a new way to predicting the effective mechanical properties for composite materials by using incompatible multivariable FEM and homogenization theory [12]. Jamal, and Mirbagheri investigated the elastic modulus of short natural fiber hybrid composites using the hybrid rule of mixture [13]. Ramesh M, Palanikumar K, Hemachandra Reddy K. evaluated the mechanical properties for the sisal-jute-glass fiber reinforced in polyester matrix composites [14]. Li, S. used two types of standardized unit cell model (Square and hexagonal) for micromechanical analysis of unidirectional composite [3]. Bonora, N. and Ruggiero, A. investigated the unit cell model development and also the effect of manufacturing process by using the micromechanical model of composites with mechanical interface [15]. Drago, A. and Pindera, M.-J. used the micro-macromechanical analysis technique for heterogeneous materials and compared the result for two cases macroscopically homogeneous and periodic micro structur.[16]. Wongsto, A. and Li, S. set up a systematic way for micromechanical analysis of UD fiber reinforced composites for random distribution of fiber [17]. To forecast the effective stiffness of fiber reinforced composites with perfect fiber orientation, the Halpin-Tsai approach is often utilized. Halpin-Tsai equations are used here for predicting transverse elastic modulus and shear modulus.

The following are the standard versions of Halpin–Tsai equations [19].

 $\frac{P}{P_m} = \frac{\left(1 + \zeta \eta v_f\right)}{\left(1 - \eta v_f\right)} \tag{1}$

$$\eta = \frac{1 + \left(\frac{P_f}{P_m}\right)}{\zeta + \left(\frac{P_f}{P_m}\right)} \tag{2}$$

In this case, P symbolizes the effective property of the composite [19,20]. Nevertheless, these procedures are not equipped to make room for the consequences of geometrical modifications of component materials at the micro level. The microscopic structure of materials directly influences their behavior in many ways. Therefore, this work aims to analyze three composite systems: random, hex-packed, and square packed to determine their effective elastic properties as well as to create glass fiber-reinforced epoxy composites with desired characteristics for specific applications by utilizing ABAQUS CAE software [21].

2.0 Computational Modeling

2.1 Governing Equation

Within the RVE macro-stresses and macro-strain are related to each other by the following equation.

$$\left\{\sigma^{M}\right\} = \left[C\right]\left\{\varepsilon^{M}\right\} \tag{3}$$

Every RVE gets applied to six different macrostrains in this procedure. For every imposed non-zero macrostrain, periodic boundary conditions typically applied to ensure that all the other macrostrains are zero [22]. The matrix [C] can be inverted to get our intended compliance matrix[S]. Compliance is the inverse property of stiffness.

$$[C]^{-1} = [S] = \begin{bmatrix} \frac{1}{E_{11}} & \frac{-\nu_{12}}{E_{11}} & \frac{-\nu_{13}}{E_{11}} & 0 & 0 & 0 & 0 \\ \frac{-\nu_{21}}{E_{22}} & \frac{1}{E_{22}} & \frac{-\nu_{23}}{E_{22}} & 0 & 0 & 0 & 0 \\ \frac{-\nu_{31}}{E_{23}} & \frac{-\nu_{33}}{E_{33}} & \frac{1}{E_{33}} & 0 & 0 & 0 & 0 \\ 0 & 0 & 0 & \frac{1}{G_{23}} & 0 & 0 & 0 \\ 0 & 0 & 0 & 0 & \frac{1}{G_{13}} & 0 \\ 0 & 0 & 0 & 0 & 0 & \frac{1}{G_{13}} \end{bmatrix}$$

$$(4)$$

2.2 Material Properties

The composite E-glass fibers are used as reinforcement within the matrix while for the matrix Epoxy resins is used. Their elastic mechanical properties are given below in a table [8].

Table 1 Elastic properties of materials.

Property	E-Glass fiber	Epoxy
Elastic modulus, E ₁₁ (GPa)	72.4	3.5
Poisson's ratio, v_{12}	0.2	0.35

2.3 Physical Aspect of the Model

For each type distribution, five RVE are designed for five distinct volume fractions of fibers (0.1, 0.2, 0.3, 0.4 & 0.5). Several fibers are taken to ensure better randomization in Random distribution. For any given fibers volume fraction,

total number of fibers can be calculated from the following equation

$$n_f = \frac{v_f A}{\pi r_f^2} \tag{5}$$

Table 2 Models for Random Distribution of Fibers.

Distribution type	Model No.	v _f	$r_f(\mu m)$	n_f
Random	01	0.1		5
	02	0.2		11
	03	0.3	8	15
	04	0.4		21
	05	0.5		26

Fig-1(a) representing the unit cell for random distribution of fibers is epoxy matrix, where the volume fraction of E-glass fibers is 0.4 or 40%. Locations for each fiber are determined by using a Python algorithm.

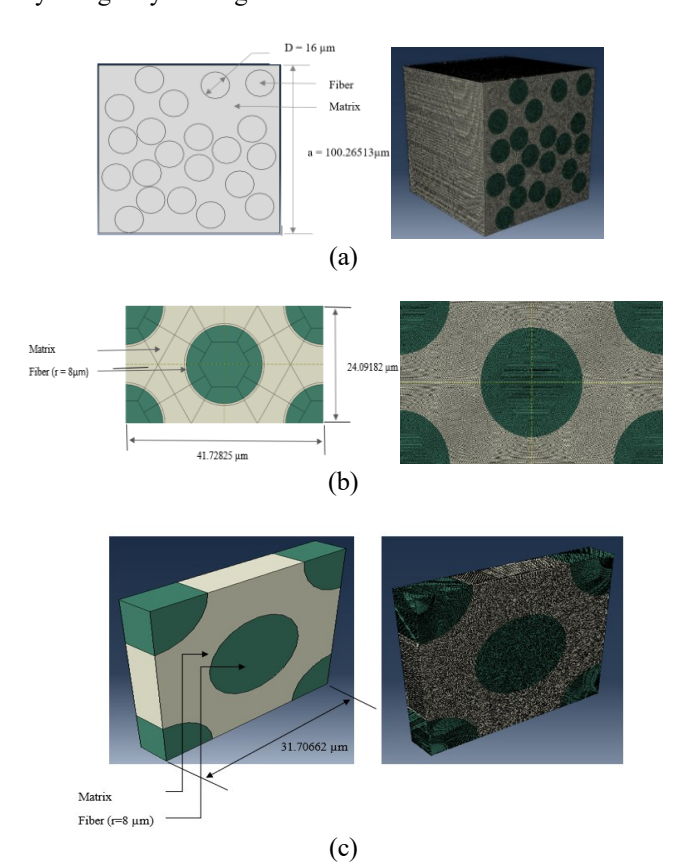


Fig. 1 Front view and meshing of model-4 for volume fraction of 0.4 (a) random (b) hexagonal and (c) square

Fig. 1(a) shows Random Distribution Model No-04 with a 40% fiber volume fraction, using hex-dominant meshing. This technique prioritizes hexahedral elements (C3D8), an 8-node linear brick element, to create high-quality meshes. Fig. 1(b) illustrates the representative volume element (RVE) where Eglass fibers are hexagonally packed, generated using a micromechanics plugin. The unit cell's dimensions are 41.72825 μm (length), 24.09182 μm (width), and 5 μm (depth), with a fiber radius of 8 μm . For square-packed fibers, the unit cell is 31.70662 μm with fibers arranged regularly. Both models assume perfect fiber-matrix interaction. Fig. 1(c) shows the

unit cell for the composite model, also meshed with C3D8 elements.

2.4 Boundary Condition

In this analysis, periodic boundary conditions (PBCs) are applied to each model. PBCs are a common technique used to approximate the behavior of an infinite or large system by analyzing a representative small portion which is known as representative volume element (RVE). This method is widely employed in finite element analysis to ensure the modeled region behaves consistently with the larger system.

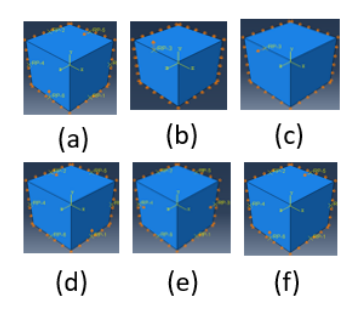
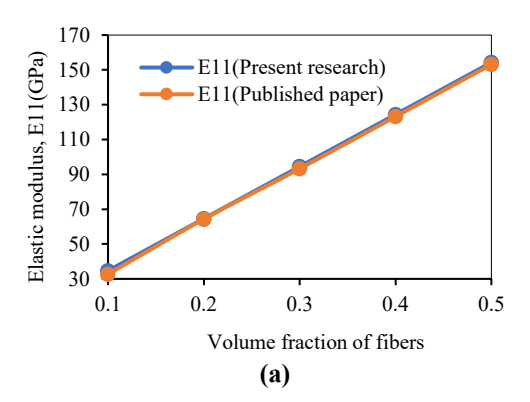


Fig.2: The displacement boundary conditions applied to determine the effective elastic characteristics are depicted schematically. (a) for E₁₁, (b) for E₂₂, (c) for E₃₃, (d) for G₁₂, (e) for G₁₃, (f) for G₂₃

2.5. Result Verification:

For accuracy of the system that is used for current work, a published research paper is chosen and verified [22].



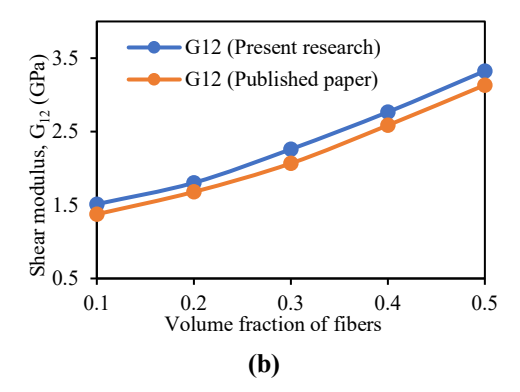


Fig.3 Comparison of current work with the work [22] for (a)longitudinal elastic property E_{11} and (b) shear modulus, G12

In Fig. 3(a) longitudinal elastic modulus from published paper and current work are compared. Shape and nature of the current study graph are perfectly agreed with the published work. Both are linearly varying with the volume fraction. From the Fig 3(b), it is noticeable that both graphs G_{12} and G_{12} (paper) have the increasing trend(non-linear) as the volume fraction increases. In most of the cases, deviation of the current work data from the published data is within 20%.

2.6 Mesh Dependency Test

Figure 4 indicates that the elastic constant E11 fluctuates below 500,000 elements, peaks at 34.651 GPa about 600,000, and then stabilizes around 1.3 million. For accuracy and minimal duration of simulation, 1 million elements are chosen as the most optimal number.

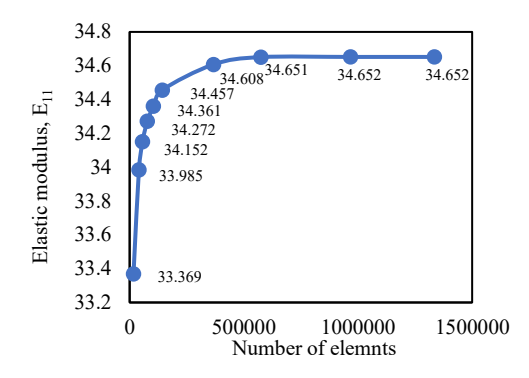


Fig.4 Variation of longitudinal elastic property E_{11} with element number.

3. Result and Discussions

3.1 Effect of Volume fraction of Fiber on Longitudinal and transverse Elastic Modulus

Random fiber distribution, from Fig.5(a), consistently achieves the maximum longitudinal elastic modulus throughout all volume fractions, from about 11.76 GPa at 0.1 volume fraction to about 39.5 GPa at 0.5 volume fraction, according to the examination of fiber distributions. This linear rise predicts improved stiffness and load transmission because the fibers are aligned favorably in numerous directions. On the other hand, an identical linear trend can be seen in hexagonal packing, where moduli gradually rise from around 10.4 GPa at 0.1 to roughly 38 GPa at 0.5. Compared to random distributions, hexagonal packing offers reasonable stiffness, but its evenly distributed organization restricts elasticity. With a starting point of around 10.53 GPa and a peak of about 38 GPa at 0.5 volume percent, square packing exhibits the lowest elastic modulus. Its lower performance can be credited to geometric arrangement-related inefficient load transmission. Elastic modulus may be approxima directly using the Rule of Mixtures (RoM):

$$E_{11} = E_f V_{fg} + E_m V_{fm}$$

which predicts values ranging from around 10.39 GPa at 0.1 to 37.95 GPa at 0.5. Fig.5(b) shows both the analytical and finite element analysis (FEA) solutions for the transverse elastic modulus E22. Unlike E11, E22 does not vary linearly. Instead, E22 shows a non-linear rising trend with the increase of volume fraction. The Rule of Mixtures (RoM) cannot accurately predict the analytical solution for E22, making it unsuitable for this task, hence a semi empirical relation named Halpin Tsai is used. The study of the transverse elastic modulus E22 as a function of volume fraction for three fiber configurations demonstrates noticeable patterns. As the volume percentage grows, the fibers start interacting more strongly, which will increase

elasticity; however, this improvement does not continue linearly due to the constraints and deformation of the surrounding matrix.

40

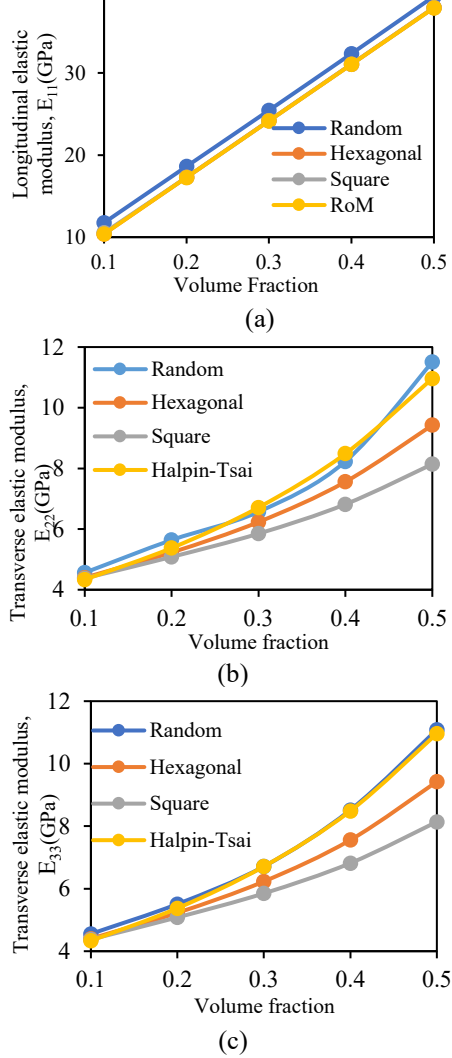


Fig.5 Effect of volume fraction of fiber on (a) longitudinal elastic modulus E11, (b) transverse elastic modulus E22 and (c) E33

At 0.1 volume fraction, the recorded E₂₂ values are as follows(approximately): Random: 4.56 GPa, hexagonal: 4.4 GPa, square: 4.35 GPa, Halpin-Tsai: 4.33 GPa. The random structure provides the better performance as compared to the square arrangement. After volume fraction of 0.3, the results vary even further. At a maximum volume fraction of 0.5, the moduli are as follows: random: 11.5 GPa, hexagonal: 9.5 GPa, square: 8.1 GPa, and halpin-tsai: 10.7 GPa. The random fiber arrangement consistently achieves the largest E22 values, with a non-linear increase as the volume percentage increases. While initially competitive, the hexagonal arrangement falls behind with increased fiber concentration, whereas the square structure stays at the lowest throughout all fractions. The Halpin-Tsai model closely resembles random behavior but tends to downplay other configurations considerably. Figure 5(c) shows that the fluctuation of E33 with respect to volume fraction follows a similar trend as that of E22. The modified Halpin-Tsai equation is used to get the analytical solution for E33, which is then compared to the FEA findings. At a volume fraction of 0.1, the moduli are: Random (4.5 GPa), Hexagonal (4.4 GPa), Square (4.37 GPa), and Halpin-Tsai (4.33 GPa). The random layout has the largest modulus, whereas the square arrangement is the least

effective. At the greatest volume fraction of 0.5, the values are: Random: 11.08 GPa, Hexagonal: 9.42 GPa, Square: 8.14 GPa, and Halpin-Tsai: 10.96 GPa. The random configuration reaches 11.0 GPa, whereas the square arrangement stays substantially lowerest. The random distribution findings correspond better with the analytical solution, but the other two configurations deviate from it. In both cases E22 and E33, fibers are aligned perpendicular to the load direction, resulting in a more complicated load transmission mechanism. At low volume fractions, the matrix material can deform greatly, and the fibers' effect on stiffness may not be completely reflected. As additional fibers are packed into the matrix, their organization and interaction can cause nonlinear effects. At a greater volume percentage, the possibility such as fiber-fiber interaction, matrix yielding, or non- uniform stress distribution might become prominent, resulting in a divergence from the linear elastic modulus change.

3.2 Effect of Volume fraction of Fiber on Poisson Ratio

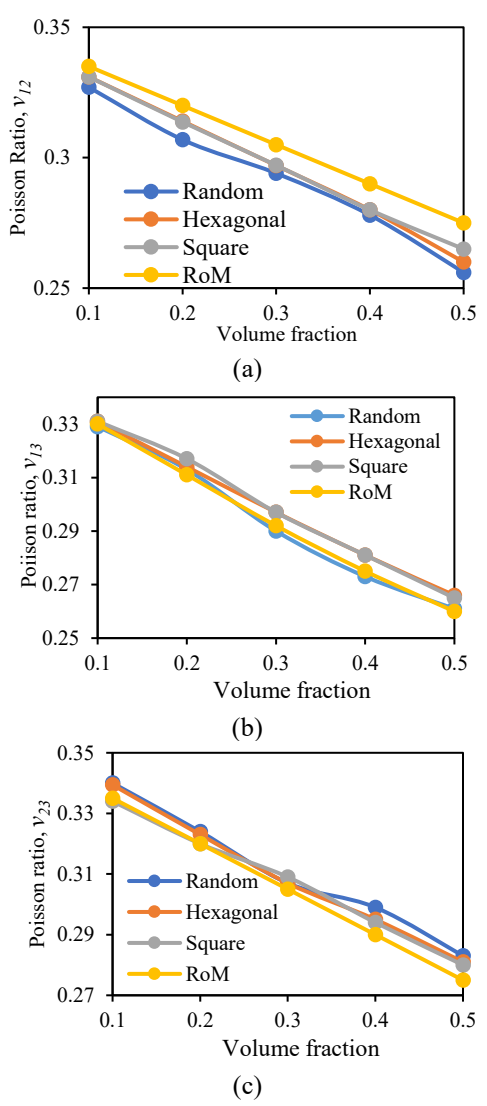


Fig .6 Effect of volume fraction of fiber on Poisson ratio, (a) v_{12} , (b) v_{13} and (c) v_{23}

Analytical solution of Poisson's ratio v_{12} , v_{13} , and v_{23} were determined with the help of Rule of mixture. Results from the Finite element analysis then compared with the analytical one obtained from role of mixture. Fig.6(a), (b), and (c) shows a declining trend for each: v_{12} , v_{13} , and v_{23} as volume fraction increases. In every case, the Rule of Mixture's

findings are in excellent agreement with the FEA solutions. As the volume fraction increases from 0.1 to 0.5, Poisson's ratio decreases across all the configurations. At a volume fraction of 0.1, the values of v_{I2} are approximately 0.32 for Random and Square, 0.33 for Hexagonal, and 0.34 for RoM. At a volume fraction of 0.5, the Poisson's ratio drops to about 0.25 for Random and Square, 0.26 for Hexagonal, and RoM. RoM as a idealized prediction remains higher than any other configuration throughout all the cases. Interaction between matrix and fiber, which is much stiffer than matrix, causes a lowering Poisson's ratio. As the volume fraction increases, fibers resist deformation more efficiently, lowering lateral strain and this leads to decreased Poisson's ratio.

3.3 Effect of Volume fraction of Fiber on Shear Modulus

First of all, analytical solutions for shear modulus are obtained using Halpin Tsai equation and then compared with the FEA solutions. Variations of G_{12} , G_{13} and G_{23} with volume fraction of fibers are showing below

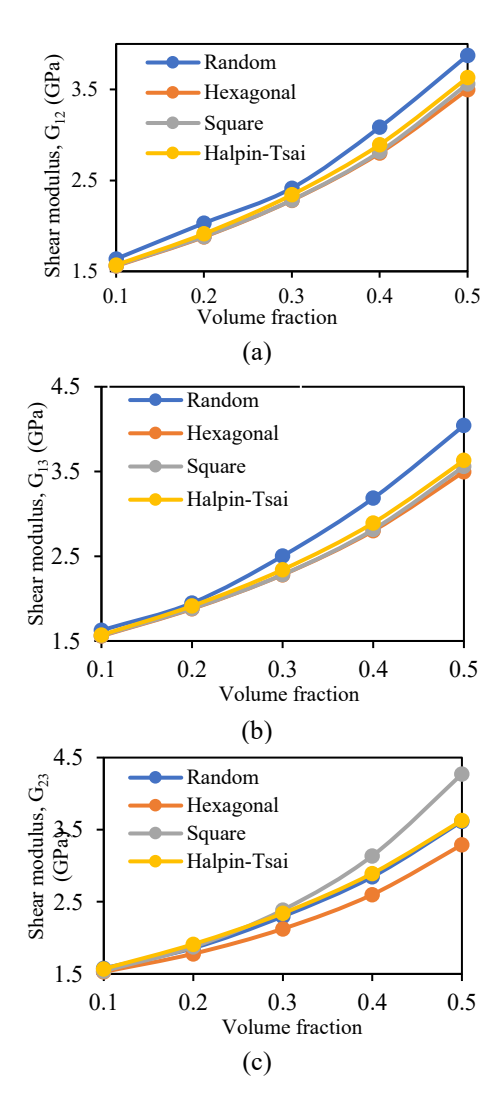


Fig.7 Effect of volume fraction of fiber on shear modulus (a) G₁₁, (b) G₂₂ and (c) G₃₃

Fig.7(a), (b) and (c) provide a comprehensive analysis of the shear modulus G_{12} , G_{13} , and G_{23} of composite materials in terms of fiber volume fraction for different configurations. Mechanical performance of these composites is compared using theoretical and empirical models such as the Halpin-Tsai equation and different fiber packing geometries. The general trend indicates that the shear modulus increases with

the fiber volume fraction for all configurations, as predicted. Results indicate that both fiber arrangement and volume fraction have a significant impact on shear modulus, with random packing providing the largest modulus values and square packing resulting in the smallest. For G_{12} , at a volume fraction of 0.1, the shear modulus is approximately 1.6 GPa, and it increases to about 3.9 GPa at a volume fraction of 0.5. The enhanced modulus for the random packing can be attributed to the more isotropic distribution of fibers, which provides a more uniform stress distribution under shear loading. The hexagonal fiber arrangement exhibited a slightly lower shear modulus compared to the random arrangement but is still significantly higher than the square packing. At a volume fraction of 0.1, the modulus is approximately 1.65 GPa, increasing to 3.5 GPa at a volume fraction of 0.5. The square fiber arrangement showed the lowest shear modulus values across all volume fractions. Initially, at low volume fractions, fiber-matrix interaction is weak, and the matrix dominates mechanical properties. At higher fiber volume fractions, interactions between fibers increase, particularly in random and hexagonal arrangements, further enhancing stiffness non-linearly.

5.0 Conclusion

The micro-mechanical modeling approach was used to investigate the homogenized mechanical properties of the epoxy composite reinforced with e-glass fibers. The influence of fiber volume fraction and arrangement on the effective elastic properties of composites has been found using for random, hex-packed, and square packed:

- Increasing the volume fraction of e-glass fibers considerably increase the elastic modulus of the composite.
- Among the three configurations (random, hexpacked, square packed), random distribution demonstrated exceptionally good alignment with the analytical solution.
- The variation of the longitudinal elastic modulus, E₁₁, was found to be linear, showing a sharp increase from 10 GPa to approximately 40 GPa as the fiber volume fraction increased from 10% to 50%.
- A similar trend was obtained for the transverse elastic moduli, E₂₂ and E₃₃, both increasing from 4 GPa to around 12 GPa as the fiber volume fraction rose from 10% to 50%.
- Poisson's ratio was found to decrease (from approximately 0.34 to 0.26) as the volume fraction of fiber increased. The overall stiffness of the composite increased with higher volume fraction which resulted in smaller lateral deformation hence the Poisson's ratio.
- Shear moduli (G₁₂, G₁₃, and G₂₃) were found to increase non linearly (roughly from 1.5GPa to 4.3GPa) as the as volume fraction of fibers went 10% to 50%.

References

[1] B. A. Bednarcyk and S. M. Arnold, "Micromechanics-based deformation and failure prediction for longitudinally reinforced titanium composites," *Compos. Sci. Technol.*, vol. 61, no. 5, pp. 705–729, Apr. 2001.

- [2] C. CHAMIS and R. LARK, "Hybrid composites State-ofthe-art review: Analysis, design, application and fabrication," Mar. 1977.
- [3] R. M. Jones, "Mechanics of Composite Materials," Oct. 2018.
- [4] C. Chamis, "Simplified composite micromechanics equations for hygral, thermal and mechanical properties | Semantic Scholar," 1983. https://www.semanticscholar.org/paper/Simplified-composite-micromechanics-equations-for-Chamis/4dc48da317971c255e9f805b44d8146f7e0065d0 (accessed May 28, 2022).
- [5] T. Mori and K. Tanaka, "Average stress in matrix and average elastic energy of materials with misfitting inclusions," *Acta Metall.*, vol. 21, no. 5, pp. 571–574, May 1973
- [6] G.-D. Cheng, Y.-W. Cai, L. Xu, G.-D. Cheng, Y.-W. Cai, and L. Xu, "Novel implementation of homogenization method to predict effective properties of periodic materials," *AcMSn*, vol. 29, no. 4, pp. 550–556, Aug. 2013.
- [7] X. Y. Zhou, P. D. Gosling, C. J. Pearce, Z. Ullah, and L. Kaczmarczyk, "Perturbation-based stochastic multi-scale computational homogenization method for woven textile composites," *Int. J. Solids Struct.*, vol. 80, pp. 368–380, Feb. 2016.
- [8] J. M. M. De Kok and H. E. H. Meijer, "Deformation, yield and fracture of unidirectional composites in transverse loading: 1. Influence of fibre volume fraction and testtemperature," *Compos. Part A Appl. Sci. Manuf.*, vol. 30, no. 7, pp. 905–916, Jul. 1999.
- [9] R. N. Yancey, "Challenges, Opportunities, and Perspectives on Lightweight Composite Structures: Aerospace Versus Automotive," *Light. Compos. Struct. Transp. Des. Manuf. Anal. Perform.*, pp. 35–52, Feb. 2016.
- [10] G. Kretsis, "A review of the tensile, compressive, flexural and shear properties of hybrid fibre-reinforced plastics," *Composites*, vol. 18, no. 1, pp. 13–23, Jan. 1987.
- [11] J. Lamon, "A micromechanics-based approach to the mechanical behavior of brittle-matrix composites," *Compos. Sci. Technol.*, vol. 61, no. 15, pp. 2259–2272, Nov. 2001.
- [12] H. Sun, S. Di, N. Zhang, and C. Wu, "Micromechanics of composite materials using multivariable finite element method and homogenization theory," *Int. J. Solids Struct.*, vol. 38, no. 17, pp. 3007–3020, Mar. 2001.
- [13] J. Mirbagheri, "(PDF) Prediction of the Elastic Modulus of Wood Flour/Kenaf Fibre/Polypropylene Hybrid Composites," 2017.
 - https://www.researchgate.net/publication/267790727_Prediction_of_the_Elastic_Modulus_of_Wood_FlourKenaf_Fibre Polypropylene_Hybrid_Composites (accessed May 28, 2022).

- [14] M. Ramesh, K. Palanikumar, and K. H. Reddy, "Mechanical property evaluation of sisal-jute-glass fiber reinforced polyester composites," *Compos. Part B Eng.*, vol. 48, pp. 1– 9, May 2013.
- [15] N. Bonora and A. Ruggiero, "Micromechanical modeling of composites with mechanical interface Part 1: Unit cell model development and manufacturing process effects," *Compos. Sci. Technol.*, vol. 66, no. 2, pp. 314–322, Feb.
- [16] A. Drago and M. J. Pindera, "Micro-macromechanical analysis of heterogeneous materials: Macroscopically homogeneous vs periodic microstructures," *Compos. Sci. Technol.*, vol. 67, no. 6, pp. 1243–1263, May 2007.
- [17] A. Wongsto and S. Li, "Micromechanical FE analysis of UD fibre-reinforced composites with fibres distributed at random over the transverse cross-section," *Compos. Part A Appl. Sci. Manuf.*, vol. 36, no. 9, pp. 1246–1266, Sep. 2005.
- [18] L. L. Faulkner *et al.*, "Principles of Composite Material Mechanics," *Princ. Compos. Mater. Mech.*, Feb. 2016.
- [19] Y. Huang, K. K. Jin, and S. K. Ha, "Effects of Fiber Arrangement on Mechanical Behavior of Unidirectional Composites:," *J. Compos. Mater.*, vol. 42, no. 18, pp. 1851– 1871, Jul. 2008.
- [20] X. Y. Zhou, P. D. Gosling, C. J. Pearce, Z. Ullah, and L. Kaczmarczyk, "Perturbation-based stochastic multi-scale computational homogenization method for woven textile composites," *Int. J. Solids Struct.*, vol. 80, pp. 368–380, Feb. 2016.
- [21] ABAQUS (2017) Analysis User's Manual, Version 6.14, Dassault Systemes, Simulia Inc.
- [22] W. J. Drugan and J. R. Willis, "A micromechanics-based nonlocal constitutive equation and estimates of representative volume element size for elastic composites," *J. Mech. Phys. Solids*, vol. 44, no. 4, pp. 497–524, Apr. 1996.

Nomenclature

 P_f : characteristics of fibers

 P_m : characteristics of matrix

 V_f : volume fraction

 ζ : geometry parameter

[C]: stiffness matrix.

 σ^{M} : macro-stress

 ϵ^{M} : macro-strain

 n_f : total number of fibers

rf: radius of fibersA: cross-sectional area